Experimental Evaluation of Feedback Modalities for Five Teleoperation Tasks

Mayez A. Al-Mouhamed[1], Mohammad Nazeeruddin[2], and Syed M.S. Islam[3]

***Abstract*— A distributed telerobotic system (DTS) is proposed based on a master arm station which is interconnected by a computer network to a slave arm station. DTS is evaluated using a set of teleoperated experiments which are (1) peg-in-hole insertion, (2) assembly of a small water pump, (3) operating drawers, (4) pouring of water, and (5) wire-wrapping. Direct teleoperation is evaluated using the following schemes: (1) stereo vision (V), (2) vision and force feedback (VFF), and (3) vision with active compliance (VAC). Space indexing and scaling tools are also used. Operator hand is logically mapped to a remote tool both in position and force. The operator feels the forces exerted on the tool as they were exerted on the hand. Extensive experimental analysis showed that mapping of operator hand motion and force feedback (FF) to a convenient tool point reduces operator mental load and task time due to highly-coordinated motion. Stereo vision may alone be used at the cost of large peak forces and extended task time. VFF has nearly equal task time as compared to VAC but with a noticeable increase in contact forces. For a large majority of cases, the contact-based tasks done using VAC resulted in the least task times and the least contact forces. VAC is superior to VFF which is better than V. In other words, there is an enormous gain in stability if one removes the bilateral force feedback channel in teleoperation and relies on a slave arm active compliance.**

***Index Terms*— Active compliance, assembly, force feedback, insertion, motion coordination, vision, teleoperation, telerobotics.**

I. INTRODUCTION

TELEROBOTICS aims at extending human natural eye-hand motion coordination over an arbitrary distance and an arbitrary scale. The objective is to replicate manipulative skills and dexterity to a remote work place. Human psychomotor skills have evolved over millions of years. The design of effective man-machine interfacing and the transmission delays are two major limiting factors [1].

A 3D virtual reality model [2], [3] of the environment is used to develop model-based assistances and mixed control modes in repeatedly performing a sequence of short modeling, programming, and execution. A virtual arm is teleoperated, while accessibility is checked, valid paths are used to control the slave arm, and feedback from slave arm is sent to control the virtual arm. The system is used in unfastening 12 nuts of a tap cover, lifting up a cover using gantry crane, inspecting the tap, and lifting down the cover and fasten it again.

(1) Department of Computer Engineering, College of Computer Science and Engineering (CCSE) King Fahd University of Petroleum and Minerals (KFUPM), Dhahran 31261, Saudi Arabia. mayez@ccse.kfupm.edu.sa

(2) Department of Systems Engineering, CCSE, KFUPM, Dhahran 31261, Saudi Arabia. nazeer@ccse.kfupm.edu.sa

(3) School of Computer Science and Software Engineering, U.W.A., Crawley, WA 6009, Australia. Email: shams@csse.uwa.edu.au

An event-driven virtual reality (VR) [4] is used to model the environment to ease the task of programming, planning, and teleoperating a remote robot. Once the VR assemblies are set up, the real links update their recorded trajectory. This approach is useful to resolve conflicts among multiple robots while reducing communication bandwidth.

In [5] a sensor-based motion-planning is proposed for teleoperation in deep space. Bilateral control of a graphic slave arm operating on a 3D graphic environment is used to select an approximate sequence of fine motions. The operator is provided with graphic animation using kinematics, dynamics, and friction. Impact forces used in a closed-loop control are used to provide the operator the feeling of repulsive forces. For this a 3D collision prevention scheme is used. The sequence is sent to a slave arm supervised by a sensor-based motion-planning algorithm and applied to a peg-in-hole assembly. Accurate graphic and physical models of slave arm and environment are needed.

Using a pre-planed insertion path, adaptive impedance control (AIC) [6] is used to reduce jamming forces by adaptively finding the desired position to follow the optimal path using the current position and environmental constraints. For peg-in-hole operations, the scheme may correct slight horizontal misalignment due to uncertainties. A two-level Teleoperation scheme [7] is proposed for the Wearable Energetically Autonomous Robot (WEAR). The master emits lower-level commands using the natural intelligence of the operator. To make decisions for the management of the robot, AI-based commands blend higher level simple commands with system and existing environmental states.

Bilateral control is one approach to replicate human performance at a remote site. Task performance can be improved [8] when force-reflection and shared compliant control are used but at the detriment of teleoperator stability. Theoretical analysis of stability/performance for position error based on Lawrence 4-channel and 5-channel schemes for teleoperation [9] indicated that a compliant slave device provides some stability advantage over a built-in passive intrinsic stiffness. Kinesthetic force feedback to the operator is helpful even under a long delay [10]. A stable bilateral teleoperator was successfully used in carrying out peg-in-hole insertion (0.4 mm clearance) and contour following while exerting a constant force under a delay of seven seconds. A gain-switching control [11] may improve the teleoperation transparency when using constant controller gains in position-error-based teleoperation during slave free motion or when colliding with a stationary stiff environment.

An anthropomorphic space robot is evaluated using kines-

thetic and stereo HMD [12]. The operator position is mapped to slave arm both in position and velocity. Evaluation of a drill task indicates less contact forces with equal task time when either visual or kinesthetic force is used with stereo vision. A mixed set of direct and task-oriented modes [13] are activated using a set of visualization and manipulation tools with some force monitoring to improve safety and accuracy in micro/nano spaces. To avoid collisions high-level motion commands are used due to electrostatic forces and possible sticking. For legged robots [14] the use of force sensing is useful to measure the foot-ground force interaction as well as the ground-reaction forces and to compute the zero-moment point in real time while standing or executing a dynamically balanced gait.

In surgery, force sensing is indispensable for reliable perception of the stiffness of soft tissue [15] to discriminate tinier differences in telemanipulation with enhanced sensitivity than through direct manipulation. The use of force feedback during micro surgeries [16], [17] indicate that typical forces on the microsurgical instrument tips during the retinal surgery are less than 7.5 mN, which is below the threshold of the operators tactile sensitivity. Unless these contact forces are properly amplified, the surgeon will not be able to sense them. Thus, the surgeon may operate with little or no tactile feedback which increases the potential of tissue damage. To measure the contact forces a miniature force sensor [16] is used at the tip of a microsurgical instrument. Position-controlled motion is proposed with micrometer resolution for force feedback of no less than 5 mN. The use of force-feedback in remote endoscopic surgery [18] proved to be beneficial. The slave manipulator quickly and accurately mimics the movement of the master arm at low speed; and the master arm satisfactorily reproduced the force. Force feedback [19] is also effective in suturing rabbits neck artery (3mm in diameter) and leg artery (1mm in diameter).

A telerobotic framework is evaluated using direct teleoperation with the following schemes: (1) stereo vision, (2) vision and FF, and (3) vision with active compliance. Indexing and scaling tools are used. The proposed system is used to carry out a set of experiments involving contact with the environment. Operator hand motion is mapped to a remote tool both in position and force. Strategies for task effective execution are discussed and presented for the experiments. Analysis of operator interaction with the environment, task time, and peak and average contact forces is presented. Comments on the global performance of each scheme is presented together with a comparison to others.

The organization of this paper is as follows. In Section 2 the telerobotic system is presented. In Section 3 the description of experimental tasks is presented. In Section 4 the used tools and strategy for the experiments are presented. In Section 5 the experimental results are presented. In Section 6 some results are compared to others. We conclude in Section 7.

II. Telerobotic System

Telerobotics allows extending eye-hand motion coordination through a computer network. Motion scaling establishes a mapping from human scale to an arbitrary target teleoperation scale (micro, nano, etc.). Telerobotics is based on developing a multi-disciplinary research environment integrating motion, vision, and haptic senses to experience manipulative tasks, system interactions, man-machine interfacing, and computer aided teleoperation (CAT). The fidelity in reproducing the tasks using different teleoperation schemes is assessed based on the analysis of some task performance metrics like peak and average contact forces and task time.

A schematic diagram of our telerobotic system is shown in Figure 1. The slave arm is a 6 dof PUMA 560. The master arm (Pending US Patent) is a light, 6 DOF, wire-based, anthropomorphic, arm that was designed and manufactured at KFUPM. The telerobotic system consists of a master arm station organized as a Telerobotic Client (TC) which is interconnected through the Internet to a slave arm station organized as a Telerobotic Server (TS). TC and TS implement (1) the bilateral master-slave interconnection at the Cartesian coordinate level, (2) motion coordination system and teleoperation tools, and (3) streaming of video data (stereo vision) and FF. The software architecture is described in [20].

In the following we shortly describe the generic impedance control implemented in the telerobotic system. At the slave arm, the joint control torque τ is used to control the arm dynamics [21]:

$$\tau = M(\theta)\ddot{\theta} + C(\theta,\dot{\theta})\dot{\theta} + G(\theta) + J_s^t(\theta)F_{ext} \qquad (1)$$

where θ, $\dot{\theta}$,and $\ddot{\theta}$ are the slave arm joint position, velocity, and acceleration, $M(\theta)$ is the inertia matrix, $C(\theta,\dot{\theta})$ is the coriolis and centrifugal matrix, $G(\theta)$ is the gravity vector, $J_s(\theta)$ is the slave arm jacobian, and F_{ext} is the external force applied at the arm tip. The control torque τ is computed as:

$$\tau = M(\theta)(\ddot{q} + K_v\,\dot{\epsilon_\theta} + K_p\,\epsilon_\theta) + C(\theta,\dot{\theta})\dot{\theta} + G(\theta) \qquad (2)$$

where q is the master arm joint position, $\epsilon_\theta = q - \theta$ the position error, and the diagonal gain matrices K_v and K_p. Note that $M(\theta)$, $C(\theta,\dot{\theta})$, and $G(\theta)$ are computed on-line by the controller. The closed loop equation is obtained by combining the above two equations:

$$\ddot{\epsilon_\theta} + K_v\,\dot{\epsilon_\theta} + K_p\,\epsilon_\theta = M(\theta)^{-1}J_s^t(\theta)F_{ext} \qquad (3)$$

The slave arm is controlled by the constant gains K_v and K_p independently from joint dependent parameters like the inertia $M(\theta)$, coriolis and centrifugal $C(\theta,\dot{\theta})$, and gravity $G(\theta)$.

The vector representing the Cartesian variation in the operator hand position and orientation is used to command the slave arm tool frame. Specifically, the master arm Cartesian velocity vector is computed as $\dot{X_m} = J_m(q)\dot{q}$, where J_m is the master arm jacobian matrix. For small variations $\dot{q}$ we have $\Delta X_m = J_m(q)\Delta q$. The variation vector $\Delta X_m = (\Delta E_m, \Delta M_m)$ consists of a translational part ΔE_m and a rotational (Euler) part ΔM_m as shown in Figure 1.

Cartesian mapping is implemented by controlling the slave arm using ΔX_m, e.g. to eliminate the structural dependence between master and slave arms. A desired joint vector q is computed for the slave arm as $\epsilon_\theta = q - \theta = J_s^{-1}\Delta X_m$ and

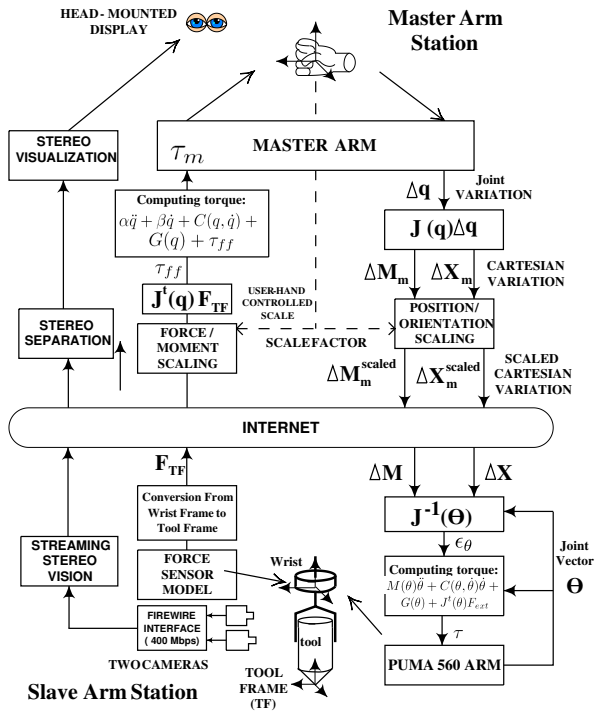

Fig. 1. Real-time transfer of motion command, force data, and live stereo video.

$q = J_s^{-1}\Delta X_m + \theta$. The above terms allow evaluating the control terms $\ddot{q}$, $\dot{\epsilon_\theta}$, and ϵ_θ that appear in Eq. 2.

Similarly, the master arm motor torque vector τ_m controls the dynamics [21] of the master arm articulated system:

$$\tau_m = D(q)\ddot{q} + C(q,\dot{q}) + G(q) \tag{4}$$

where q is master arm joint angular vector, $D(q)$ is the inertia matrix, $C(q,\dot{q})$ is the coriolis and centrifugal coefficients, and $G(q)$ is the gravity vector. This allows computing terms $C(q,\dot{q})$ and $G(q)$ based on the dynamic model of the master arm. The inertia matrix $D(q)$ is nearly constant for a light master arm operating in a restricted work volume.

The force measured at the slave arm tool is to be displayed at the operator hand center. For this, the master arm controller computes the torque vector τ_m as follows:

$$\tau_m = \alpha\ddot{q} + \beta\dot{q} + C(q,\dot{q}) + G(q) + \tau_{ff} \tag{5}$$

where term $\alpha\ddot{q}+\beta\dot{q}$ is generated based on the operator motion, terms $C(q,\dot{q})$ and $G(q)$ are used to compensate for dynamic effects and gravity, and τ_{ff} is the reflected FF torque. Torque τ_{ff} is induced by the slave arm force vector F_{TF}, expressed in the tool frame (TF), but measured by a wrist force sensor as shown on Figure 2. In other words $\tau_{ff} = J_m^t(q)F_{TF}$. At the master station, F_{TF} is scaled (magnified) by the operator using the master arm as a pointer to some pre-defined scale in the stereo picture displayed on the HMD. More details about force conversion can be found in [22]. The overall dynamic motion equation becomes:

$$F_{TF} = J^{-t}(q)(\,(\alpha - D(q))\ddot{q} + \beta\dot{q}) \tag{6}$$

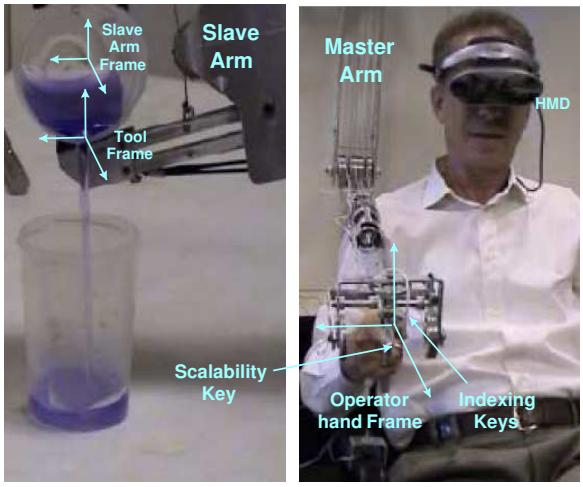

Fig. 2. Operator hand frame is logically mapped to a user-defined slave arm tool frame. Also shown operator Head-Mounted Display (HMD), Scalability and Indexing control keys.

where term $\alpha - D(q)$ represents the reduced master arm inertia and $\beta\dot{q}$ is a damping factor. The motivation for injecting term $\alpha\ddot{q} + \beta\dot{q}$ in the master arm torque is to reduce overall mechanical impedance felt by the operator. The values of the parameters α and β are experimentally determined. The above equation allows displaying on the operator hand the force vector F_{TF} computed in the slave arm tool frame.

In the following Section, we present the experimentation details by considering the task description and specifications.

III. Task Description and Specification

In this section we describe the experimental part of a multi-threaded distributed component framework for telerobotics. In the following sub-sections experiments are presented with their geometric and mechanical specifications.

A. Peg-in-hole insertion

The objective is to expose the proposed framework to an operation involving the following aspects: (1) teleoperation with kinesthetic FF display at the master arm or with active compliance at the slave station, (2) logical mapping of operator hand motion to a floating tool frame TF attached to a peg, (3) use of available computer-aided teleoperation (CAT) tools. Insertion deals with grasping of a peg, moving it to the top of hole, detecting contact with the hole, and inserting the peg in hole. The geometric dimensions, clearance, and chamfer geometry are shown on Figure 3-(a). For smooth insertion, the peg tip was rounded and the hole was chamfered. To avoid damaging the robot and sensors the hole was attached to a 1 kg base for which the sideways movements are permitted in response to a lateral force exceeding 8 N.

B. Assembly of a pump

This assembly requires a high-degree of eye-hand motion coordination with balanced dependence on both vision and FF. In the studied case the assembly operation requires two objectives to be met at the same time. The mechanical tolerance

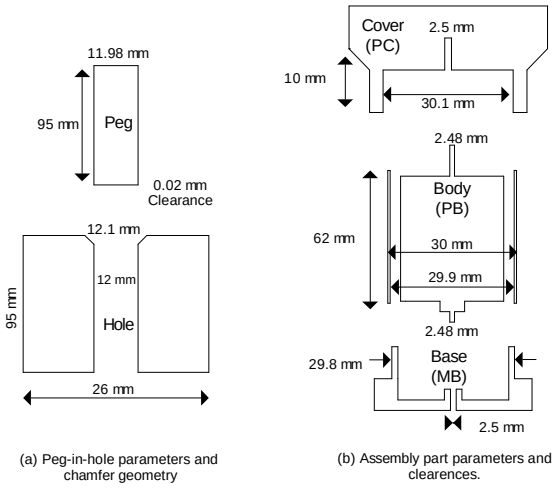

(a) Peg-in-hole parameters and chamfer geometry

(b) Assembly part parameters and clearences.

Fig. 3. Features and parameters of the peg-in-hole and pump components

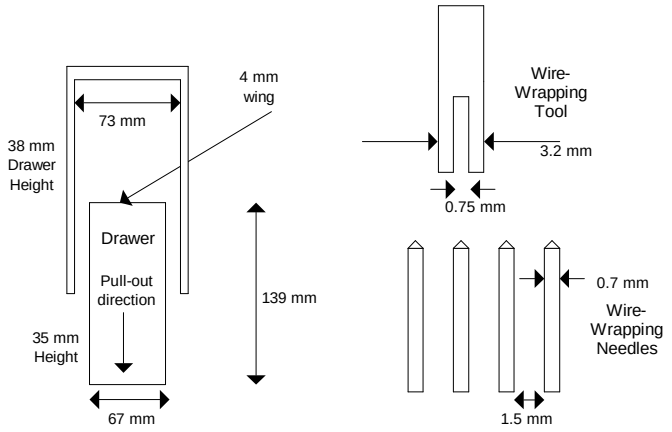

(a) Drawer parameters

(b) Parameters of Wire-wrapping needles and tool

Fig. 4. Dimensioning parameters of drawers and wire-wrapping experiments

of the parts is relatively moderate as compared to that of the peg and the hole. These are shown on Figure 3-(b). A car water pump is used to carry out assembly and disassembly operations. The pump consists of three cylindrical parts: (1) a plastic cover (PC), (2) a metallic base (MB), and (3) a pump body (PB) which contains a motor to be assembled in the middle of the above two parts. The motor shaft axis appears on both top and bottom sides of PB. Initially MB is attached to a fixed platform for which the sideways movements are permitted in response to a lateral force exceeding 8 N. MB can be tilted by up to an angle of 10 degrees with respect to horizontal plane. The task is to grasp PB, move it to top side of fixed MB and carry out part mating of PB and MB. Then the above operations are repeated to assemble PC on the top on PB-MB compound.

C. Operating drawers

The task of operating drawers requires a high-degree of eye-hand motion coordination with moderate use of FF. The used drawer has a small vertical wing at its end to block its

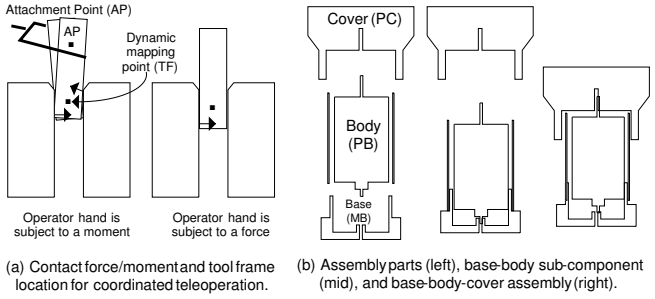

(a) Contact force/moment and tool frame location for coordinated teleoperation.

(b) Assembly parts (left), base-body sub-component (mid), and base-body-cover assembly (right).

Fig. 5. Strategy used for peg-in-hole insertion and assembly of a water pump.

entire retrieval by only sliding it outward. Once it reaches the blocking position at its end, the removal of the drawer requires (1) tilting it upward to free its bottom, and (2) sliding it downward to free its top. Figures 4-(a) shows the specification of the drawer used.

D. Pouring

The objective is to expose the proposed framework to the following aspects: (1) teleoperation with fine trajectory and time control, (2) extensive use of eye-hand motion coordination, (3) perception of 3D scene and scene depth, (4) evaluation of functional and ergonomic aspects of proposed CAT tools. This task deals with grasping of a small cup that contains colored water using the slave arm gripper, moving it to the neighborhood of an empty cup, and pouring the water in the target cup.

E. The wire-wrapping operations

The objective is to evaluate performance of the proposed teloperation system in a scaled-down slave arm space. The task is to insert the head of the wire-wrapping tool into a series of needles of a wire-wrapped electronic circuit. The operation must repeat from one needle to next in a row of 5. Figures 4-(b) shows the specification of the wire-wrapping gun and needles.

IV. Experimental methodology

In this section we describe the computing configuration prior to addressing the analysis of experimental results.

The TS and TC are run on two PCs having 2-GHz Intel P4 processors with 1GB DRAM and 512 KB cache memory and run MS Window 2000. Programs are written in MS Visual C# with the above .NET framework. Each PC is attached to a campus network by using a 100 Mbps NIC card. The server PC is interfaced to two Sony Handycam digital cameras using a 400 mbps FireWire PCI card. The client PC uses an NVIDIA display adaptor to interface with an SVGA resolution Cy-visor 3D Head-Mounted Display (HMD).

The sampling rate of 120 Hz is achieved for FF and 50 Hz for operator commands. Stereo video transfer operates at a rate of 17 fps. Total reference delays for force and stereo are 8 ms and 83 ms, respectively. Overall round-trip system delay between client and server is 183 ms (5.5 Hz) when slave arm is operated at 10 Hz, excluding delays caused by the

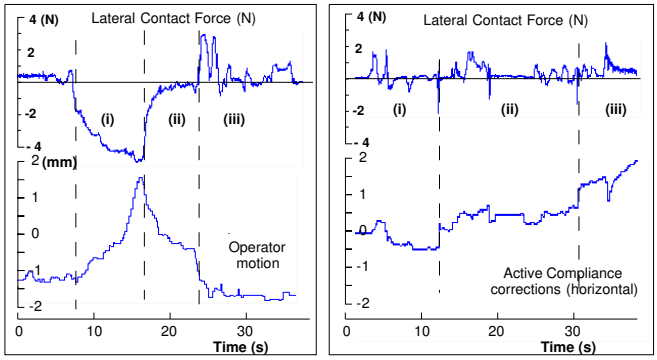

(a) Insertion using Force Feedback VFF: (i) Approaching in direction of constraints, (ii) Sliding on Surface, and (iii) Insertion while searching to zero force in opposite direction.

(b) Insertion using Active Compliance VAC: (i) approaching hole and contact, (ii) Sliding on Surface while avoiding constraints, (iii) and Insertion: progress in depth, and contact with hole bottom.

Fig. 6. Insertion using VFF (a) and VAC (b).

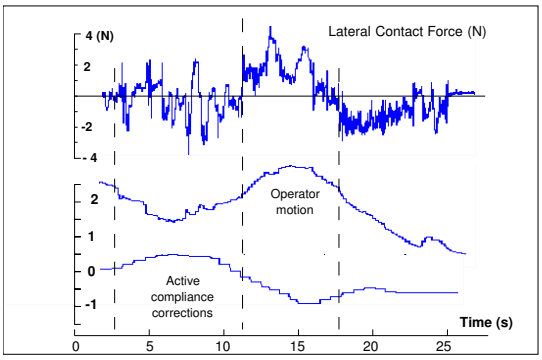

Fig. 7. Insertion using VFFAC.

operator. The above delays represents the ”best effort” from the simultaneous streaming of video, commands, and force data over a campus network using MSF C# programming and .NET Remoting. The characterization of delays, delay jitter, and scattered distribution of video, commands, and force can be found in [22] and [23]. Video clips on these experiments can be found at [24].

In the next subsections the task strategy, experimental analysis, and results are presented.

A. *Peg-in-hole insertion*

The peg-in-hole insertion consists of searching an unconstrained motion path in a space constrained by the jamming force and moment (F/M). The peg is held by the slave arm gripper. To start, the peg is held in the axial direction of the hole to the best of operator and the stereo vision system. The displayed 6D FF represents the forces exerted on the slave arm tool to which the peg is firmly attached. Here stereo vision perception provides coarse information while displayed FF is critical to search unconstrained motion directions based on correcting both peg-hole axial and rotational mismatches.

Consider a mapping scheme (S1) for which the variation in the operator hand position and orientation is used to command the slave arm attachment point (AP) shown on Figure 5-(a). At the server, the force measured at AP of slave arm is computed and displayed, in the client station, at the operator hand center. Thus the operator hand is mapped to AP by both position and force. Here the stereo vision is not very helpful in making fine translational or rotational motion corrections. Since the operator hand is logically mapped to the peg at point AP, a single F/M contact component corresponds to a subset of coupled F/M being sensed by the operator at AP which might defeat the operator action to nullify the above F/M by simple hand motion. We found that it is difficult for a human to comprehend an F/M vector, applied to hand, as opposed to a single F/M component. Therefore setting the motion mapping should be guided by the need to uncouple contact F/M in an attempt to reduce the operator mental load and operation time. For this mapping S-1 was abandoned due to lack of efficiency.

Another mapping (S-2) consists of initially setting the mapping point at the edge of the peg and dynamically compute the new mapping point by locating it in the middle of the peg part that is already inserted in the hole as shown on Figure 5-(a), e.g. point TF. This can be evaluated using (1) the horizontal plane at the top of the hole which is taken as reference for zero depth and (2) current peg depth. This strategy aims at capturing the jamming F/Ms where they are exerted on the peg and display them on the operator hand to favor direct corrections of both peg-hole misalignment errors (moment) and translational errors (force). Hence the objective of this mapping is to logically map the operator hand at a point where it is: (1) effective to capture the mechanical constraints such as the jamming forces, and (2) easy to make necessary correction through motion mapping. Since the above point is dynamically re-mapped to the operator hand motion, thus, the operator rotational and translational corrections are likely to reduce the above constraints due to the one-to-one mapping of the jamming constraints and the corrective motion done by the operator. The scaling function is used here to scale-down the operator motion in all directions to allow fine (1) motion correction in the horizontal plane, and (2) controlling the force exerted by the peg on the hole. Visual monitoring is also used to appreciate the progress in the insertion.

Figures 6-(a) and (b) show performance of peg-in-hole insertion using VFF and VAC teleoperation schemes. The upper and lower plots correspond to displayed FF and operator motion command, respectively. These interactions are exchanged through the network. In step (i) of VFF, the operator searches an unconstrained motion path in a space constrained by a contact force (-4 N), e.g. a wall effect. In step (ii), operator changes direction and reduces lateral contact force which allows the peg to go deeper in the hole. In step (iii), a different contact force appears and the same cycle is repeated until completion of insertion.

The third approach (S-3) consists of a supervisory corrective motion done by the local force controller and the remote slave arm. This solution is similar to the second mapping in terms of measurement of mechanical constraints at the above floating TF point but instead of forwarding contact F/M to the operator, active compliance controller is activated at the slave station (shorter loop) which leads to superimpose locally computed peg motion corrections (rotational and axial corrections) to

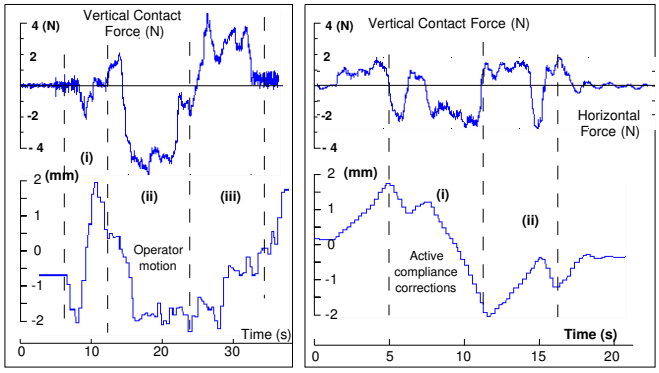

(a) Assembly using force feedback VFF: (i) Approaching pump-base and contact, (ii) Sliding on Surface (part mating of body-base), and (iii) removal of body.

(b) Assembly using active compliance VAC: (i) Approaching by pushing (operator) downward for part mating with AC corrections, and (ii) operator removes body and reaction of AC.

Fig. 8. Assembly using VFF (a) and VAC (b).

motion instructed by the operator. In this case the operator may limit his control of the peg to the vertical direction with the corresponding FF. The space scaling function is used here to scale-down the operator motion in the horizontal plane (10:1) with a unit scale in the insertion direction which allows the operator to control the vertical force the peg is exerting on the hole.

In Figure 6-(b) an active compliance control is set at the server. The upper and lower plots correspond to displayed contact force which is measured at the server and the motion correction made by the active compliance controller, respectively. These interactions are local to the slave station. The operator applies a downward force (step (i)) while active compliance control searches a horizontal position and orientation (step (ii)) that reduces contact F/M components. Due to the mapping of tool F/M to operator hand, components are likely to be uncoupled from each other and corrected independently from each other. This results in the lowest exposure to contact forces.

An experimental setting for vision, FF, and active compliance (VFFAC) teleoperation scheme is shown for the case of the insertion on Figure 7. VFFAC leads to excessive system instability evidenced by the large jamming force magnitude and interaction frequencies observed on the plot of the force as compared to the interaction forces of VFF and VCC schemes shown on Figure 6. This excessive force magnitude is expected because in VFFAC there are two independent and uncoordinated corrective processes: the local AC and remote operator, which are concurrently controlling the slave arm tool. The other undesirable effect is the delay time: the AC controller immediately reacts to measured tool F/M, while the operator sees and feels the FF with the above delays. This leads inevitably to some coupled corrections destabilizing the teleoperation system. Due to the above reasons scheme VFFAC is not found to be useful.

B. Assembly of a water pump

The assembly plan is as follows. PB is grasped and moved to the vicinity of MB. Operator carries out axis alignment to the best of the available depth perception. The steps are shown on Figure 5-(b). Part mating requires meeting two constraints which are (1) force contact of the motor shaft axis and insertion in the middle hole of MB, and (2) part mating of both lateral cylinders of PB and MB while maintaining axes alignment. The above constraints must be met in a sequential order starting with the best possible configuration that can be achieved using stereo vision and later combining both FF and visual information. Similar operation is carried out for assembling PC on the top on PB-MB compound.

The assembly strategy consists of using a balanced mixing of visual and FF in addition to space scaling to maintain some geometric directions and keep correcting other references. Specifically the visual feedback is used to establish a proper geometric setting in the pre-positioning phase. The operator space mapping in the horizontal plane is scaled down, for example by a factor of 10:1, to maintain the part positioning and to limit potential motion in the horizontal plane. The vertical axis is left with unit scale under operator control. This approach allows preserving axis alignment (first constraint) of the parts during the part mating operation (second constraint). It allows the operator carrying out fine force control in pushing one part into another while monitoring the results. In the case of large positioning errors or axis misalignment during the part mating operation, the tool is lightly lifted up (failure) and the space scaling is increased (for example to 3:1). Correction of part position and orientation are made before attempting again the part mating phase. FF is critical in carrying out the part mating in which the part is subject to a soft downward push under careful visual monitoring using zoomed stereo vision for the early detection of potential mismatch. In summary, successful part mating is based on a combination of fine FF control and depth perception in addition to the use of button-controlled tools like indexing and scaling.

Figures 8-(a) and (b) show performance of assembly tasks schemes VFF and VAC, respectively. Under VFF scheme, in step (i) PB is moved by the operator to MB where a contact force is detected. Pre-positioning and part mating are performed in step (ii). A sharp change in the displayed force causes a wall effect, e.g. resist to motion. In step (iii) PB is extracted from the assembly with a release FF and return to zero force once in free air. The fluctuations in force are caused by the friction.

In Figure 8-(b) the sensed contact force is used by the active compliance to carry out corrections of position and orientation of PB while the operator attempts the part mating. Part mating is performed in step (i). Notice the resulting FF when the part hits the bottom of MB. In step (ii) PB is extracted from the assembly with an additional release FF and returns to zero force once in free air. The contact forces involved have less magnitude and duration than those of the VFF scheme.

C. Operating drawers

The drawer is pulled up until its top wing reaches the blocking point. During the above operation motion scaling can be used to scale down the operator motion in all directions except the pulling direction to maintain directional motion. The blocking end is detected using both visual and FF.

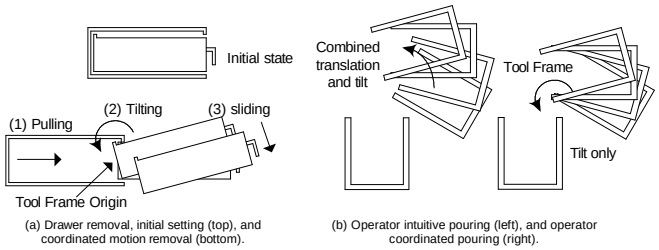

(a) Drawer removal, initial setting (top), and coordinated motion removal (bottom).

(b) Operator intuitive pouring (left), and operator coordinated pouring (right).

Fig. 9. Strategy used for operating a drawer and pouring water

To ease the task, the operator hand is to be mapped to a point TF located at end of the drawer so that the needed tilt operation can be made using a rotation about the horizontal axis at TF. Figure 9-(a) shows the initial closed drawer (up) and the steps for its opening and entire removal (down). For this, the GUI, AR tools, and master arm are used to point to the new TF origin O_{TF}. This allows relocating TF. Now the operator hand motion maps logically to TF and the contact F/Ms are now computed with respect to TF before being forwarded to the operator or locally used in the slave active compliance loop. This provides one of the best possible logical mapping from the operator hand to manipulated object so that the needed action is projected on one single axis at the new location of TF. In other words, the operator feels the contact between the wings with the environment as if the drawer is held by the operator. By tilting the hand in the upward direction the front side of drawer is tilted up which frees the drawer bottom that can now be shifted downward before becoming entirely free. During the above operations the contact forces displayed on the operator hand (master arm) are very helpful in detecting potential contacts that may result from errors in the location of TF and implied operator motion.

D. Pouring

The pouring operation consists of (1) grasping, (2) traveling, and (3) pouring. Grasping requires the slave arm to move down to a pre-apprehension configuration prior to grasping of a cup (FC) filled with colored water. The operator (in the loop) tries to center the jaw to middle of FC at its mid height to avoid potential collision. During grasping the indexing function is frequently used to maintain the master arm within a small operator dexterity area whenever the motion requires moving along a path consisting of a long translation or rotation. Traveling requires lifting FC and moving towards the target cup (TC) while maintaining the slave gripper in a horizontal plane and progressively setting up of FC orientation when approaching TC. Pouring requires setting up a proper pre-pouring configuration in the vicinity of TC. Now FC must be tilted while keeping its top above TC. This normally consists of a rotation and a translation as shown on Figure 9-(b-left). To reduce the workload on the operator it is more interesting to relocate the mapping function of the slave tool at one of the top lateral point of TC which becomes the origin of the new TF. In this case tilting the operator hand leads to directly tilting the new TF about one axis of above frame as shown on Figure 9-(b-right). We note that placing TF origin (and orientation) at the above critical point contributed in reducing the task time by about 40% as compared to default setting of TF at gripping point. In addition, it helped the operator predicting the tool path occupancy during the hand-tool mapping. The above mapping provided an ergonomic teleoperation tool because it helped minimizing the number of iterations for setting the tool in a given configuration.

E. The wire-wrapping operations

The GUI is used to set up (1) scale level of FF, and (3) the camera zooming level. The space scaling is directly controlled by the operator index. The converging setting consists of scaling the operator motion by a factor of 30:1, the FF by a factor of 1:10, and stereo camera zooming by a factor of 1:40. The operator moves the wire-wrapping tool (WWT) while aligning its axis with the circuit needle using stereo vision and carries out the insertion. The operator needs to feel the vertical force component to avoid damaging the needle during contact because actually only a small central hole in WWT must fit the needle as shown on Figure 4-(b). In this case the operator carries out corrections of axis mis-alignment, and (2) insert WWT head in the needle. The distance between two needles is about 1.5 mm. The above task was successful in making five successive insertions in a line in 30 seconds. The operator adaptation to working with some small scale appeared to be smooth and simple. Multiple zooming views is useful to avoid changing the zooming level whenever axis alignment needs correction.

V. Results and Discussion

In this section we present (1) the results of using the proposed telerobotic system in performing peg-in-hole insertion and assembly tasks, and (2) recommendations on how to improve the man-machine interfacing. These tasks are selected because they require effective interaction between the operator and the remote task involving fine motion, FF, and stereo vision. The results are limited to the period of interactions with the environment such as the insertion phase in peg-in-hole operation and the part mating phase in the assembly operation. Both phases follow the contact detection phase. We study the following teleoperation schemes in which the operator has control of a 6 DOF master arm and working with the above teleoperation schemes (V, VFF, and VAC).

Each of the insertion and part mating phases was carried out by 12 students aged between 18 and 24. The designer explained to them the various aspects of the telerobotic system for 2 hours. The objective function is to carry out the above two tasks in the least possible time while minimizing contact forces to reduce potential damage and improve teleoperation effectiveness. The objective function was carefully explained and discussed to the students. Each student was allowed to experience the insertion and assembly tasks at least 10 times before recording the data. Thus the initial learning period for each operator is between one to two hours.

Each operator carried out the insertion and assembly tasks using V, VFF, and VAC teleoperation schemes. Each scheme was carried out 12 times in total for each of the above two

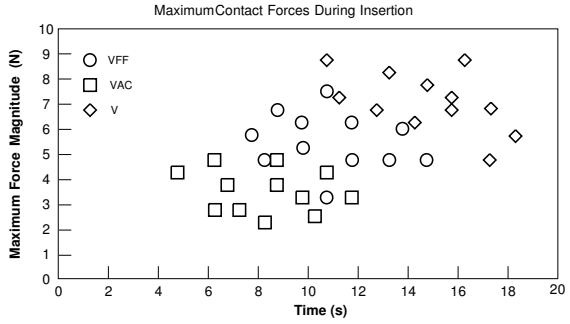

Fig. 10. Maximum insertion forces with respective task times

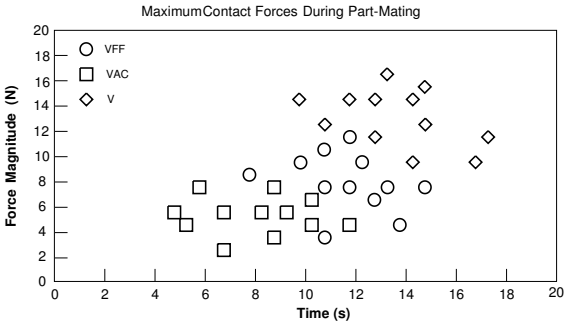

Fig. 12. Maximum assembly forces with respective task times

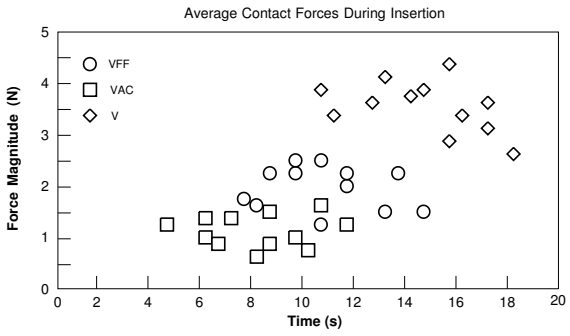

Fig. 11. Average insertion forces with respective task times

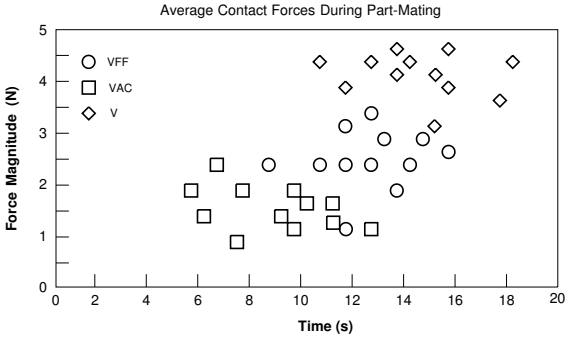

Fig. 13. Average assembly forces with respective task times

phases. The collected data refers to maximum and average F/M magnitudes as well as the corresponding completion time of a given operation for a given operator. In total we have 72 plots for two phases. The F/M vectors are all computed at the origin of reference TF. Since F/M vector has six components, each component contains qualitatively similar information in terms of peak and average force and time dependence on the operator or AC controller corrections. Combined results for all operators are presented.

Figures 10, 11, 12, and 13 show the maximum and average force exerted during peg-in-hole insertion and assembly versus task time, respectively. The operators were satisfied with the quality of stereo vision provided during the experiments. Stereo vision is one critical augmentation in telerobotics. Generally, scheme V allows completion of the insertion but with the largest contact forces and completion times as compared to the other schemes. Occasionally V scheme may produce less contact forces and possibly less duration than the other two schemes. Table I shows the ratio of maximum and average force and task time for V and VFF over VAC. The use of only visual feedback for any operator makes it longer and harder to correct axis misalignment. Thus peak and average forces dominate in V as compared to the other schemes as shown on Table I. The average force indicated some dependence on the operator speed and overall performance for a given operator. The ranking of operator performance is mainly the same in each scheme.

With VFF the operator is part of a force-position loop. Operator feels the contact F/M exerted on the remote slave tool and reacts by searching for a tool position and orientation which zeros F/M. The average force magnitude and task time shown in Table I for both insertion and assembly indicate that VFF significantly contributed in reducing the contact forces throughout the task execution that were experienced under the V scheme.

On the other hand, VFF and VAC have comparable task times. However, VFF results in a noticeable increase in contact forces as compared to VAC as shown on Table I. As the operator is part of the force-position loop under VFF, delays cause some loop instability which were shown on the FF component in Figures 6(a) and 8(a). The instability contributes in degrading overall teleoperation performance as compared to a slave arm implementing a local active compliance, e.g. VAC. This is evidenced in the FF component shown in Figures 6(b) and 8(b) and by the ratio VFF/VAC shown in Table I. For a large majority of cases, the contact-based tasks that were carried out using VAC resulted in the least contact forces and least task times. One may conclude that active compliance loop at the server station is better prepared to react to contact forces than the remote operator. This shows the efficiency of the supervisory approach and its local active compliance that continuously searches to nullify the external F/M by correcting tool position and orientation at current TF. Occasionally VAC gets higher times due to temporary blocking caused by excessive vertical force commanded by the operator.

Referring to Table I, teleoperation with VAC is still ranked first but with less advantages in the assembly as shown for the average force and task time. The reason is probably due to operator ability to combine FF with vision perception in the critical phases of the part mating. In both insertion and

	Force Magnitude		Task Time
Performance Ratio	Maximum	Average	duration
V/VAC for Insertion	1.93	3.85	1.76
VFF/VAC for Insertion	1.45	1.89	1.33
V/VAC for Assembly	2.33	2.74	1.55
VFF/VAC for Assembly	1.27	1.63	1.36

TABLE I
RATIO OF FORCE MAGNITUDE AND TASK TIME FOR V AND VFF VS. VAC.

assembly, VAC contributed in reducing peak and average contact forces as compared to both V and VFF schemes especially in the case of the insertion. VAC equally reduced the task time for each of the VFF and V schemes in both insertion and assembly tasks.

Some of the major sources of fatigue are: (1) the difficulty to comprehend and interpret 6 D vector F/M, and (2) the eyes stress caused by extensive use of stereo vision. Operators were able to comfortably work between 1 to 2 hours with an acceptable level of fatigue.

Telerobotics needs advanced supervisory tools that embed complex force and position control with dynamic motion/force mapping. Effective man-machine interfacing is needed to integrate the above tools in a simple and natural way at the operator index and stereo space. The stereo space visible to the operator and its AR capabilities need to support the above integration. The connectivity between master and slave arms can be temporarily switched off and master arm used as a 3D pointer. A variety of AC scenarios can be associated graphical features in the operator stereo space. These can be selected and grouped in AC compounds (ACCs) as task-oriented and operator favored tools. To activate a specific ACC at the task point of interest, the operator can use the master arm to point to a given ACC in stereo space, drag it, change its orientation, drop it at a desired tool point, and control its activation. This allows composing optimized ACC mechanisms and efficiently activating them at the right location and orientation with respect to current task.

VI. COMPARISON TO OTHERS

In virtual reality based teleoperation [2], [3], [4], [13] the operator plans an operation using a model, the plan controls a slave arm, and slave arm transmits back parametric feedback. The primary issue is operation safety. Mainly off-line approaches are used and teleoperation is carried out on a static environment with no dynamic interaction reported. However, in [5] graphic animation of robot kinematics, dynamics, friction, and impact forces used in a closed loop control provides the operator the feeling of repulsive forces which allowed to carry out peg-in-hole insertion. The proposed telerobotic framework provides direct-oriented teleoperation with CAT tools augmented with some supervisory control schemes to improve teleoperation effectiveness in real interactions with the environment.

We concur with [10] on the importance of kinesthetic FF in assembly operations. We extended direct teleoperation by using compliance control that makes the slave arm continuously searching to nullify F/M sensed on the current tool while the whole arm is being driven by the operator to take advantage of the above mechanism in the current task. In comparison to [6] our proposed VFF and VAC schemes have similar effects in modifying task trajectory. The active compliance controller continuously produces corrections in tool position and orientation that reduce tool external F/M. Operator sets task-oriented compliance and leads the arm under compliance equilibrium to work location. Proposed VAC reduced peak contact forces and task time as compared to kinesthetic FF with vision in insertion and assembly tasks. VAC may also be useful as a task locality mechanism to ensure task continuity in delayed teleoperation. We use constant controller gains in the dynamic controller for which the gain-switching technique proposed in [11] may improve sensitivity and transparency especially in the case of contact with rigid, elastic, or tissue objects.

The wrench mapping of [12] is comparable to proposed tool motion and force mapping. However, our dynamic mapping scheme proved to be useful tool for many tasks where the point of interest is function of task state. Proposed mapping makes the operator logically mapped, in position and force, to the remote object. In addition we proposed indexing and scaling tools and a tool-oriented dynamic motion mapping in position and force to carry out coordinated motion as a strategy to reduce operator cognitive load. This enables force reflection from current tool to the operator which increases the feeling of telepresence and enables teleoperation tasks to be completed more easily and with lower contact forces. The successful accomplishment of the above experiments is fundamentally due to the proposed dynamic mapping scheme which is estimated to be the most critical CAT tool in proposed telerobotics.

We presented extensive experimental analysis showing that VAC is superior to VFF which is better than V. It is important to notice the gain in stability which is observed on Figures 6 and 8 when switching from VFF to VAC. There is an enormous gain in stability if one removes the bilateral force feedback channel in teleoperation and relies on a slave arm active compliance.

VII. CONCLUSION

A set of assembly tasks have been used to evaluate a client-server telerobotic system which transfers motion, FF, and stereo vision over a network. The tasks are (1) peg-in-hole insertion, (2) assembly of a pump, (3) operating drawers, (4) pouring of water, and (5) wire-wrapping. The operator has been provided with (1) stereo vision V, (2) vision and force feedback VFF, and (3) vision and active compliance VAC. Active compliance has been used as assistance to direct

teleoperation in addition to indexing and scaling tools. A dynamic mapping of operator hand motion and force to a task-oriented tool point has been used to reduce operator cognitive load and task time. Button-controlled indexing and scaling proved to be the most frequently used tools. Scaling was useful to operate in a 30:1 scaled down space as well as a linear dimension blocking tool. Scheme V allowed to complete the above tasks but resulted in the largest contact forces and task times as compared to VFF and VAC. In contact centric tasks, like insertion, VAC noticeably outperforms V and VFF and provides task quality control. In multi-objective tasks, like assembly, VAC and VFF are closer in peak and average force as well as in task times. However, VFF results depend more on operator skills. There is an enormous gain in stability if one removes the bilateral force feedback channel in teleoperation and relies on a slave arm active compliance. Teleoperation modality with VAC control is useful for extending human eye-hand motion coordination and dexterity to a remote workplace in hazardous, hostile, un-accessible, and small-scale environments.

VIII. Acknowledgement

This work is supported by King Abdulaziz City for Science and Technology (KACST) under grant AT-20-80 and King Fahd University of Petroleum and Minerals (KFUPM).

References

[1] D.E. Whitney. Historic perspective and state-of-the art in robot force control. *The Inter. J. of Robotics Research*, 6:1:3–14, 1987.

[2] E. Even, P. Gravez, E. Maillard, and E. Fournier. Acquisition and exploitation of a 3D environment model for computer aided tatleloperation. *Proc. of the 1999 IEEE Inter. Workshop on Robot and Human Integration*, pages 261–266, Sep. 1999.

[3] E. Even, E. Fournier, and R. Gelin. Using structural knowledge for interactive 3D modeling of piping environments. *Proc. of IEEE Inter. Conf. on Robotics and Automation*, pages 2013–2018, Apr. 2000.

[4] Bailin Cao, G.I. Dodds, and G.W. Irwin. An event driven virtual reality system for planning and control of multiple robots. *Proc. IEEE/RSJ Int. Conf. on Intelligent Robots and Systems, 1999. IROS '99*, 2:1161–1166, Oct. 1999.

[5] N. Funabiki, K. Morishige, and H. Noborio. Sensor-based motion-planning of a manipulator to overcome large transmission delays in teleoperation. *Proc. IEEE Int. Conf. on Systems, Man, and Cybernetics, 1999. IEEE SMC '99*, 5:1117–1122, Oct. 1999.

[6] Sukhan Lee, Ming-Feng Jean, Jong-Oh Park, and Chong-Won Lee. Reference adaptive impedance control: a new paradigm for event-based robotic and telerobotic control. *IEEE/RSJ International Conference on Intelligent Robots and Systems, 1998*, 2:1302 – 1307, Oct. 1998.

[7] S.C. Jacobsen, M. Olivier, F.M. Smith, D.F. Knutti, R.T. Johnson, G.E. Colvin, and W.B. Scroggin. Research robots for applications in artificial intelligence, teleoperation and entertainment. *The International Journal of Robotics Research*, 23(4-5):319–330, 2004.

[8] W.S. Kim, B. Hannaford, and A.K.; Fejczy. Force-reflection and shared compliant control in operating telemanipulators with time delay. *IEEE Trans. on Robotics and Automation*, 8:2, 1992.

[9] Goran A. V. Christiansson and Frans C. T. van der Helm. The Low-Stiffness Teleoperator Slave – a Trade-off between Stability and Performance. *The International Journal of Robotics Research*, 26(3):287–299, 2007.

[10] T. Imaida, Y. Yokokohji, T. Doi, M. Oda, and T. Yoshikwa. Ground-space bilateral teleoperation experiment using ETS-VII robot arm with direct kinesthetic coupling. *Proc. of the IEEE Int. Conf. on Robotics and Automation,ICRA 2001*, 1:1031 – 1038, June 2001.

[11] Liya Ni and David W. L. Wang. A Gain-Switching Control Scheme for Position-Error-Based Bilateral Teleoperation: Contact Stability Analysis and Controller Design. *The International Journal of Robotics Research*, 23(3):255–274, 2004.

[12] L.E.P. Williams, R.B. Loftin, H.A. Aldridge, E.L. Leiss, and W.J. Bluethmann. Kinesthetic and visual force display for telerobotics. *IEEE Inter. Conf. on Robotics and Automation, ICRA '02*, 2:1249–1254, 2002.

[13] A. Codourey, M. Rodriguez, and I. Pappas. A task-oriented teleoperation system for assembly in the microworld. *Proc. 8th International Conference on Advanced Robotics, 1997. ICAR '97*, pages 235–240, July 1997.

[14] Hector Montes, Samir Nabulsi, and Manuel A. Armada. Reliable, built-in, high-accuracy force sensing for legged robots. *The International Journal of Robotics Research*, 25(9):931–950, 2006.

[15] G. De Gersem, H. Van Brussel, and F. Tendick. Reliable and enhanced stiffness perception in soft-tissue telemanipulation. *The International Journal of Robotics Research*, 24(10):805–822, 2005.

[16] P.J. Berkelman, L.L. Whitcomb, R.H. Taylor, and P. Jensen. A miniature microsurgical instrument tip force sensor for enhanced force feedback during robot-assisted manipulation. *IEEE Trans. on Robotics and Automation*, 19:5:917–921, Oct. 2003.

[17] J. Arata et al. Development of a dexterous minimally-invasive surgical system with augmented force feedback capability. *2005 IEEE/RSJ Int. Conf. IROS*, pages 3207–3212, 2005.

[18] A. Matsui, K. Mabuchi, T. Suzuki, A. Namiki, M. Ishikawa, H. Fujioka, and H. Ishigaki. Development of a remotely-operated master-slave manipulation system with a force-feedback function for use in endoscopic surgery. *IEEE Inter. Conf. on Eng. in Medicine and Biology*, 2:1260 – 1263, July 2000.

[19] S. Wang et al. A robotic system with force feedback for micro-surgery. *Proc. 2005 IEEE Int. Conf. on Robotics and Automation*, pages 199–204, 2005.

[20] M. Al-Mouhamed, O. Toker, and A. Iqbal. A multi-threaded distributed telerobotic framework. *IEEE Trans. on Mechatronics*, 11(5):558–566, October 2006.

[21] J.P. Desai and R.D. Howe. Towards the development of a humanoid arm by minimizing interaction forces through minimum impedance control. *Proc. IEEE International conference on Robotics and Automation, ICRA*, 4(2):4214 – 4219, 2001.

[22] M. Al-Mouhamed, M. Nazeeruddin, and N. Merah. Design and analysis of force feedback in telerobotics. *To appear in the IEEE Trans. on Instrumentation and Measurements*, 2008.

[23] M. Al-Mouhamed, O. Toker, and A. Iqbal. Performance evaluation of a multi-threaded distributed telerobotic framework. *Submitted for publication*, December 2008.

[24] Video clips. *http://www.ccse.kfupm.edu.sa/researchgroups/robotics3*.